Geometry of Coordinatively Unsaturated Two-Legged Piano Stool Complexes with 16 Valence Electrons: A Theoretical Study†

Thomas R. Ward,*,‡ Olivier Schafer,§ Claude Daul,§ and Peter Hofmann*,⊥

Organisch-Chemisches Institut der Universität Heidelberg, Im Neuenheimer Feld 270, D-69120 Heidelberg, Germany, Departement für Chemie und Biochemie der Universität Bern, Freiestrasse 3, CH-3012 Bern, Switzerland, and Institut für anorganische Chemie der Universität Freiburg, Pérolles, CH-1700 Fribourg, Switzerland

Received January 23, 1997⊗

The structure of coordinatively unsaturated (16-electron) two-legged piano stool complexes is analyzed with the extended Hückel methodology as well as with density functional theory. Pyramidal, and thus potentially chiral at the metal, geometries are predicted to be preferred for complexes bearing ligands like CO, CS, or NO^+, containing low-lying π-acceptor orbitals, as well as in the case of electropositive strong σ donors, e.g., for silyl ligands. In all cases, however, the computed inversion barriers are low (<15 kcal mol^{-1}). A minimum was located for an η^2-coordination of an acyl ligand in $[CpFe(acyl)NO]^+$, which may account for the stereospecific ligand substitution in acyl-containing systems. The ground-state geometry of the isoelectronic series $[(\eta^n\text{-}C_nH_n)M(CO)_2]$ (M = Fe, Mn, Cr, V; n = 4−7) is probed as a function of ring size and metal center.

Introduction

Although the possibility of metal-based chirality was demonstrated nearly 100 years ago by Werner,[1] Brunner gave it a new impetus as he initiated a systematic study of pseudotetrahedral chiral three-legged piano stool complexes.[2,3] Compounds of the type $[CpML^1L^2L^3]$ (Cp = cyclopentadienyl) are chiral at the metal and can be resolved in many cases if an element of chirality is introduced either on one of the ligands L, on the Cp ring, or as a counterion. After diastereomer separation, the enantiopure resolving agent may be removed, affording a chiral at metal compound.

Over the years, a number of groups have studied such complexes and their use in organic transformations. Elegant applications come from the groups of, among others, Brunner,[3−5] Davies,[6,7] Faller,[8−14] and Gladysz.[15−21,41] To the best of our knowledge, however, such chiral at metal compounds have only found stoichiometric, and not catalytic, applications in organic chemistry.

Recently, organometallic compounds with a d^6 electron count have been used as Lewis acid catalysts in C−C bond-forming reactions, e.g., in Diels−Alder and Mukaiyama reactions.[22−29] The perspective of using a piano stool complex seems very appealing in this respect. However, it is imperative to ensure configurational stability of the catalyst, as racemization of the latter would have a dramatic effect on the enantiomeric excess of the product. Therefore, we have undertaken a theoretical study of the configurational stability of pyramidal vs planar coordinatively unsaturated two-legged piano stool (half-sandwich) complexes $[CpML^1L^2]$ with a 16 valence electron count. These, being generated from an appropriate chiral $[CpML^1L^2L^3]$ precursor and acting as a Lewis acid, would be either intermedi-

† Dedicated to Professor Walter Siebert on the occasion of his 60th birthday.
‡ Universität Bern.
§ Universität Freiburg.
⊥ Universität Heidelberg.
⊗ Abstract published in *Advance ACS Abstracts,* June 15, 1997.

(1) Werner, A. *Ber. Dtsch. Chem. Ges.* **1911**, *44*, 1887.
(2) Brunner, H. *Angew. Chem., Int. Ed. Engl.* **1969**, *8*, 382; *Angew. Chem.* **1969**, *81*, 395.
(3) Brunner, H. *Adv. Organomet. Chem.* **1980**, *18*, 151.
(4) Brunner, H.; Aclasis, J.; Langer, M.; Steger, W. *Angew. Chem., Int. Ed. Engl.* **1974**, *13*, 810; *Angew. Chem.* **1974**, *81*, 864.
(5) Brunner, H.; Fisch, K.; Jones, P. G.; Salbeck, J. *Angew. Chem., Int. Ed. Engl.* **1989**, *28*, 1521; *Angew. Chem.* **1989**, *101*, 1558.
(6) Davies, S. G. *Pure Appl. Chem.* **1988**, *60*, 13.
(7) Davies, S. G. *Aldrichim. Acta* **1990**, *23*, 31.
(8) Faller, J. W.; Lambert, C.; Mazzieri, M. R. *J. Organomet. Chem.* **1990**, *383*, 161.
(9) Faller, J. W.; Linebarrier, D. L. *J. Am. Chem. Soc.* **1989**, *111*, 1937.
(10) Faller, J. W.; Linebarrier, D. L. *Organometallics* **1990**, *9*, 3182.
(11) Faller, J. W.; Nguyen, J. T.; Ellis, W.; Mazzieri, M. R. *Organometallics* **1993**, *12*, 1434.
(12) Faller, J. W.; Ma, Y. *Organometallics* **1992**, *11*, 2726.
(13) Faller, J. W.; Mazzieri, M. R.; Nguyen, J. T.; Parr, J.; Tokunaga, M. *Pure Appl. Chem.* **1994**, *66*, 1463.
(14) Schilling, B. E. R.; Hoffmann, R.; Faller, J. W. *J. Am. Chem. Soc.* **1979**, *101*, 592.
(15) Merrifield, J. H.; Fernández, J. M.; Buhro, W. E.; Gladysz, J. A. *Inorg. Chem.* **1984**, *23*, 4022.
(16) Fernández, J. M.; Gladysz, J. A. *Inorg. Chem.* **1986**, *25*, 2672.
(17) Dalton, D. M.; Garner, C. M.; Fernández, J. M.; Gladysz, J. A. *J. Org. Chem.* **1991**, *56*, 6823.
(18) Klein, D. P.; Gladysz, J. A. *J. Am. Chem. Soc.* **1992**, *114*, 8710.
(19) Dalton, D. M.; Fernández, J. M.; Emerson, K.; Larsen, R. D.; Arif, A. M.; Gladysz, J. A. *J. Am. Chem. Soc.* **1990**, *112*, 9198.
(20) Bodner, G. S.; Smith, D. E.; Hatton, W. G.; Heah, P. C.; Georgiou, S.; Rheingold, A.; Geib, S. J.; Hutchinson, J. P.; Gladysz, J. A. *J. Am. Chem. Soc.* **1987**, *109*, 7688.
(21) Wang, Y.; Gladysz, J. A. *J. Org. Chem.* **1995**, *60*, 903.
(22) Bonnesen, P. V.; Puckett, C. L.; Honeychuck, R. V.; Hersh, W. H. *J. Am. Chem. Soc.* **1989**, *111*, 6070.
(23) Bach, T.; Fox, D. N. A.; Reetz, M. T. *Chem. Commun.* **1992**, 1634.
(24) Kündig, E. P.; Bourdin, B.; Bernardinelli, G. *Angew. Chem., Int. Ed. Engl.* **1994**, *33*, 1856; *Angew. Chem.* **1994**, *106*, 1931.
(25) Hollis, T. K.; Odenkirk, W.; Robinson, N. P.; Whelan, J.; Bosnich, B. *Tetrahedron* **1993**, *49*, 5415.
(26) Odenkirk, W.; Whelan, J.; Bosnich, B. *Tetrahedron Lett.* **1992**, *39*, 5729.
(27) Odenkirk, W.; Rheingold, A. L.; Bosnich, B. *J. Am. Chem. Soc.* **1992**, 6392
(28) Faller, J. W.; Smart, C. J. *Tetrahedron Lett.* **1989**, *30*, 1189.
(29) Faller, J. W.; Ma, Y.; Smart, C. J.; DiVerdi, M. J. *J. Organomet. Chem.* **1991**, *420*, 237.

S0276-7333(97)00036-8 CCC: $14.00

ates or transition states in a catalytic process. One of us[30] has published a preliminary account of this work, focusing upon extended Hückel (EH) model calculation, for the carbonyl-substituted half-sandwich intermediate $[CpMn(CO)_2]$, which was shown to possess a pyramidal ground-state geometry.[31−33] This quite common, synthetically useful fragment is routinely produced by photolysis of $[CpMn(CO)_3]$ and has been investigated in matrix isolation studies.[34−36] Model calculations for related systems with different types of ligands L^1, L^2 and for $\{(\eta^7\text{-}C_7H_7)V\}$, $\{(\eta^6\text{-}C_6H_6)Cr\}$, and $\{(\eta^4\text{-}C_4H_4)Fe\}$ as metal templates, all isoelectronic to the $\{(\eta^5\text{-}C_5H_5)\text{-}Mn\}$ moiety, showed that the geometry of such 16 valence electron species is not only intimately related to the donor nature of L^1 and L^2 but also depends upon the metal center and the ring size of the η^n-bound C_nH_n cyclopolyene ring in the general case $[(\eta^n\text{-}C_nH_nML^1L^2]$.[37] Although most of the results presented here are based upon EH calculations, two relevant cases have also been studied with the density functional methodology in order to reach more reliable absolute energy assignments. Computational details are presented in the Appendix.

Results and Discussion

Pure σ Donors as Ligands. As representative models for chiral, pyramidal $\{CpML^1L^2\}$ fragments with potential configurational stability we consider half−sandwich complexes derived from the conical d^6 metal template $\{CpFe\}^+$, and we first built the MOs of this fragment, which we will be using extensively in our analysis.[38] The three filled π-orbitals of the Cp^- system (a_2'', e_1'') have a strong overlap with the metal orbitals, while the empty e_2'' set has δ-symmetry with respect to the M−Cp axis and, therefore, only interacts weakly with the metal. The resulting interaction diagram is presented in Figure 1. The a_2'' orbital interacts mostly with the sp hybrid on the metal, the degenerate d_{yz} and d_{xz} set interacts efficiently with the e_1''; their out-of-phase combination being the LUMO for a d^6, 12 electron system. As the d_{z^2} orbital interacts weakly with the a_2'' orbital of the cyclopentadienyl, it is slightly destabilized with respect to the $d_{x^2-y^2}$ and d_{xy}, both of δ symmetry. Therefore, the d_{z^2} is the HOMO, and the HOMO−LUMO gap is 1.5 eV for the $\{CpFe\}^+$ fragment, Figure 1.

The simplest two-legged piano stool we consider contains two extra hydrides simulating pure σ donors in $[CpFeH_2]^-$. As a starting point, we set these in the *yz* plane. As the rotation barrier of the cyclopentadienyl ligand is too small to be computed accurately within our framework, we consider these "planar" two-legged piano stool complexes as C_{2v}-symmetric. The symmetric

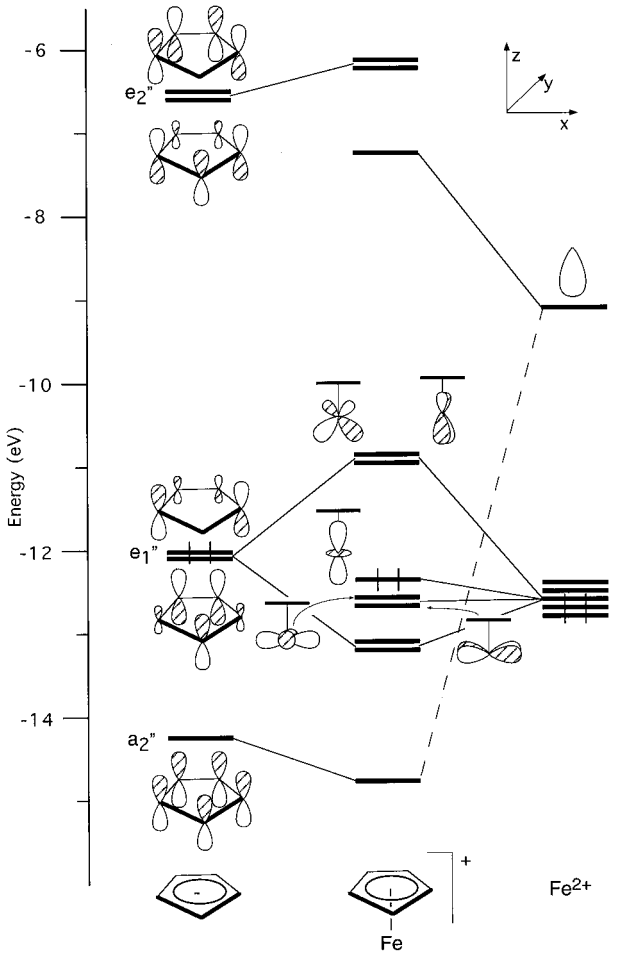

Figure 1. Simplified interaction diagram between Cp^- and Fe^{2+}.

combination σ_s of the two 1s donor orbitals of the hydride ligands interacts mostly with the empty sp hybrid MO of the $\{CpFe\}^+$ but also in a slightly destabilizing manner with both the $d_{x^2-y^2}$ and d_{z^2} fragment MO's of the metal fragment, which, through the intervention of the σ_s, undergo orbital mixing (i.e., intrafragment polarization of the two formerly orthogonal MOs of $\{CpFe\}^+$ occurs). The HOMO can therefore be described in terms of perturbation theory as $[d_{x^2-y^2} - \sigma_s + d_{z^2}]$ with, however, only a minimal contribution from the σ_s orbital (vide infra). The antisymmetric group orbital σ_a interacts with the d_{yz} orbital, removing the degeneracy of the LUMO of $\{CpFe\}^+$, leaving behind the d_{xz} MO of $\{CpFe\}^+$ as the LUMO of the dihydride complex. With a 1.4 eV HOMO−LUMO gap in our EH calculations, the molecule should be stable in this geometry, Figure 2.

The goal of this study is to find out how to force a two-legged piano stool complex $[CpFeL^1L^2]$ into a pyramidal and, thus, chiral arrangement. We may turn the question around and study the requirements that would make the achiral planar $[CpFeL^1L^2]$ geometry an unstable one relative to a chiral, pyramidal structure. This relates to the question of which electronic properties of ligands L^1 and L^2 could stabilize the HOMO and destabilize the LUMO of a $[CpFeL^1L^2]$ molecule in the sense of a second-order Jahn−Teller distortion. The Jahn−Teller second-order theorem predicts that for a small HOMO−LUMO gap there exists a distortion of $\Gamma_{HOMO} \otimes \Gamma_{LUMO}$ symmetry that opens up the gap and

(30) Hofmann, P. *Angew. Chem., Int. Ed. Engl.* **1977**, *16*, 536; *Angew. Chem.* **1977**, *89*, 551.
(31) Bursten, B. E.; Gatter, M. G. *J. Am. Chem. Soc.* **1984**, *106*, 2554.
(32) Fitzpatrick, N. J.; Rest, A. J.; Taylor, D. J. *J. Chem. Soc., Dalton Trans.* **1979**, 351.
(33) Johnson, T. J.; Folting, K.; Streib, W. E.; Martin, J. D.; Huffmann, J. C.; Jackson, S. A.; Eisenstein, O.; Caulton, K. G. *Inorg. Chem.* **1995**, *34*, 488.
(34) Herberhold, M.; Kremnitz, W.; Trampisch, H.; Hitam, R. B.; Rest, A. J.; Taylor, D. J. *J. Chem. Soc., Dalton Trans.* **1982**, 1261.
(35) Caulton, K. G. *Coord. Chem. Rev.* **1981**, *38*, 1.
(36) Black, J. D.; Boylan, M. J.; Braterman, P. S. *J. Chem. Soc., Dalton Trans.* **1981**, 673.
(37) Hofmann, P. Habilitationsschrift, Universität Erlangen, 1977.
(38) Elian, M.; Chen, M. M. L.; Mingos, D. M. P.; Hoffmann, R. *Inorg. Chem.* **1976**, *15*, 1148.

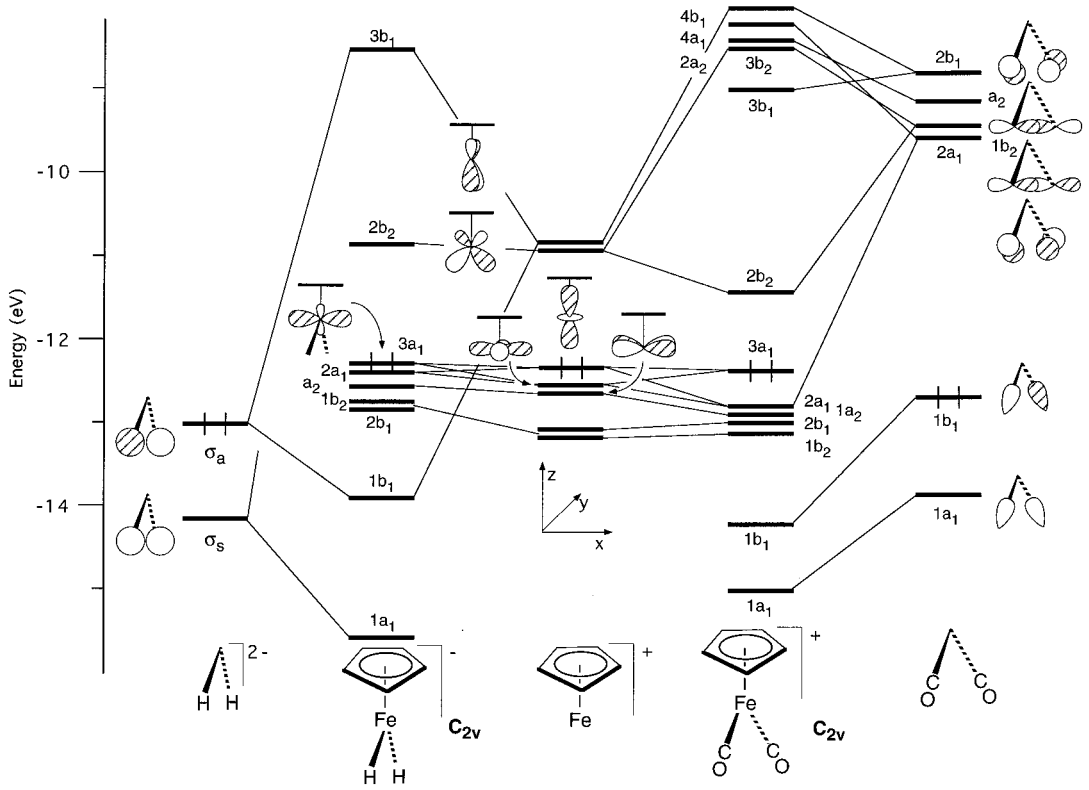

Figure 2. Simplified interaction diagram between H_2^{2-} and $CpFe^+$ (left) and $CpFe^+$ and $(CO)_2$ (right) in a planar (C_{2v}) geometry.

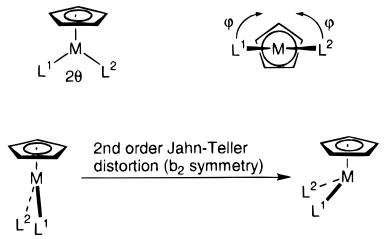

Figure 3. Defining the variables for the Jahn−Teller distortion.

stabilizes the system.[39] In the case of our simple, pure σ-donor model $[CpFeH_2]^-$, the distortion $\Gamma_{HOMO} \otimes \Gamma_{LUMO} = b_2$ indeed corresponds to a rotation in opposite directions of both hydride−metal bonds around the z axis, pyramidalizing the system (Figure 3). We will therefore analyze the frontier orbital situation of the general $[CpFeL^1L^2]$ case with respect to its ligand-dependent tendency to undergo this planar to pyramidal geometry change for a series of prototypical ligands.

Unless stated otherwise, in all the EH calculations, we optimized the L−M−L angle 2θ for the planar geometry, and then while keeping the L−M−L angle constant, the rotation angle around the z axis φ was optimized. For specific $[CpML_2]$ cases, two-dimensional energy surfaces $E = E(\theta,\varphi)$ were computed, optimizing simultaneously the angle θ between the M−L vectors and the z-axis as well as the pyramidality angle φ. Along the distortion pathway shown in Figure 3, the system undergoes a descent in symmetry from C_{2v} (planar) to C_s (pyramidal), which allows for considerable mixing of molecular orbitals. For a more general case $[CpFeL^1L^2]$, where L^1 and L^2 are different, the pyramidal geometry is C_1-symmetric and thus is chiral.

(39) Albright, T. A.; Burdett, J. K.; Whangbo, M.-H. *Orbital Interactions in Chemistry*; John Wiley: New York, 1985.

Table 1. Gradient-Corrected DFT Geometry Optimization of $[CpFeH_2]^-$

R(Fe−H) (Å)	1.525	φ (deg)	0
$R(Cp_{centroid}-Fe)$ (Å)	1.680	θ (deg)	58.5

Next, we computed the distortion of $[CpFeH_2]^-$ along the angular coordinate φ. Since the hydrides contribute only minimally to the HOMO and not to the LUMO, these MOs are left nearly unperturbed. The HOMO, due to its large energy separation from the lowest unoccupied level, is only very slightly stabilized by mixing into itself the LUMO wavefunction. While going down in symmetry, the σ_s combination mixes in (out-of-phase) with the d_{xz} orbital, slightly destabilizing the LUMO. The same argument, however, applies for the filled d_{xy} orbital, which upon distortion mixes (out-of-phase) with σ_a and becomes destabilized. The total energy profile for the distortion follows closely the fate of this orbital. The planar starting geometry with both σ donors in the yz plane is favored because the destabilization of the occupied frontier MOs (mainly d_{xy}) by far overcomes the minimal energy gain caused by the second-order Jahn−Teller stabilization of the HOMO.

Full optimization of the model $[CpFeH_2]^-$ with density functional theory calculations (DFT, see the Appendix for details) confirms that the ground-state geometry is indeed planar (Table 1), with a remarkable H−Fe−H angle ($2\theta = 117°$). Very similar values were obtained both at the LDA and gradient-corrected levels of theory.

For somewhat more realistic models of $CpML_2$ systems with "pure σ donors" as ligands, e.g., for the 16-electron bis-phosphine complexes $[CpMn(PH_3)_2]$ and $[CpFe(PH_3)_2]^+$, we find that these are also predicted to adopt planar geometries. For the $\{PH_3\}_2$-fragment (only 3s,3p valence AOs, no 3d functions on P), we compute σ_s, the in-phase combination of the two phosphine lone-

pair donor MOs, to lie at −15.19 eV. Like σ_s in the bis-hydride case, this fragment orbital does not contribute noticeably to the HOMO of the complexes and σ_a of $(PH_3)_2$ does not mix into the d_{xz} LUMO. The resulting wide HOMO−LUMO gaps of ca. 1.4 eV for the $[CpMn(PH_3)_2]$ and $[CpFe(PH_3)_2]^+$ complexes again favor a planar geometry over the pyramidal one in both cases.

As mentioned above, close inspection of the HOMO of planar $[CpFeH_2]^-$ reveals that it can be described as resulting from a three-orbital interaction $[d_{x^2-y^2} - \sigma_s + d_{z^2}]$ with some additional s and p_z component from the sp-hybrid of $\{CpFe\}^+$ at the metal center. The σ_s fragment orbital (computed at −14.11 eV, somewhat higher in energy than σ_s of the $(PH_3)_2$ ligand set) contributes only about 3% to the HOMO of $[CpFeH_2]^-$. According to the rules of second-order perturbation theory, lowering the ionization potential (raising the orbital energy) of the σ donors, i.e., going less electronegative, better σ-donating ligands, will increase the σ_s contribution to the HOMO. As the σ_s linear combination mixes into the HOMO of the complex in an out-of-phase manner from below, stronger σ donors should raise the HOMO. This, in turn, increases the second-order Jahn−Teller-based tendency to pyramidalize, eventually forcing a complex $[CpFeL^1L^2]$ with two pure and very good σ donors to adopt a pyramidal geometry in its ground state.

This qualitative reasoning was tested computationally by replacing hydride ligands in $[CpMnH_2]^{2-}$ (1s orbital energy −13.6 eV) by hydride-like model donor ligands X^- that carried a single 1s-type donor function and two electrons, but that had their orbital energy set at −12.0 eV. For these better σ donors and for a fixed value of θ = 54°, a pyramidal structure of $[CpMnH_2]^{2-}$ with φ = 25° is lower in energy than the planar geometry by approximately 5 kcal mol^{-1} (0.21 eV).

As silanes are electropositive ligands, we studied the bis-silyl complex $[CpFe(SiH_3)_2]^-$ as a model system containing two realistic good σ donor ligands. The in-phase combination of the lone pairs σ_s of two SiH_3^- is computed at −10.98 eV, while the out-of-phase combination lies at −7.95 eV. In this case, the σ_a combination lies so high in energy that its bonding combination with the d_{yz} orbital becomes the HOMO (−11.71 eV, $2b_1$). The σ_s now contributes 51% to the HOMO-1 (−11.76 eV, $2a_1$, practically degenerate with the HOMO). The LUMO (−10.85 eV, $2b_2$) is, as before, the nonbonding d_{xz} orbital of b_2 symmetry. The computed HOMO−LUMO gap is 0.86 eV, considerably smaller than for $[CpFeH_2]^-$. However, $\Gamma_{HOMO} \otimes \Gamma_{LUMO} = a_2$ does not correspond to a pyramidalization distortion. The HOMO-1 orbital, has a_1 symmetry and is only 0.91 eV away from the LUMO and corresponds in character to the HOMO levels discussed before. The small gap between HOMO-1 and LUMO allows for pyramidalization via a distortion of b_2 symmetry. The effect is only small: we compute the pyramidal geometry to be only 0.94 kcal mol^{-1} (0.04 eV) more stable than the planar one, which indicates extremely shallow energy barriers for distortion.

From these σ donor case studies, we conclude that 16 electron $[CpML_2]$ or $[CpML^1L^2]$ piano stool complexes containing ligands L with pure or predominant σ-donor properties will have a planar geometry, or at most may be slightly pyramidalized for very good σ donors, but the inversion barrier is so small that they most certainly invert in solution even at very low temperature.

***π* Ligands: *π* Acceptors.** The presence of empty or filled p, or d, or π orbitals on the ligands L should have a pronounced effect upon the HOMO−LUMO gap because the empty d_{xz} orbital (LUMO) can participate in a π-type interaction with the ligands L, which are either π acceptors or π donors.

Choosing a system with empty orbitals of π symmetry should serve our purpose: the LUMO, a more or less pure {CpM} d_{xz} orbital without ligand contributions in the pure σ donor case, will be stabilized upon interaction and thus lie closer in energy to the HOMO. A second-order Jahn−Teller distortion of b_2-symmetry should become more favorable as a consequence of a reduced HOMO−LUMO gap and pyramidalize the system. On the right side of Figure 2 we present an interaction diagram for planar $[CpFe(CO)_2]^+$. As can be seen, the d_{xz} orbital interacts efficiently with the b_2 combination of the π*-orbitals of the $\{CO\}_2$ fragment. The in-phase combination with d_{xz} is the LUMO of planar $[CpFe(CO)_2]^+$, while the d_{z^2} mixes with the $d_{x^2-y^2}$ orbital and remains the HOMO. For a planar $[CpFe(CO)_2]^+$ system we compute a HOMO−LUMO gap of 0.9 eV.

Upon pyramidalization, the $1b_2$ combination of p_x orbitals on the $\{CO\}_2$ fragment mixes considerably with the HOMO, contributing to its stabilization. On the other hand, the LUMO, which is M−(CO) bonding, is destabilized as the HOMO mixes-in, hybridizing the metal orbital away from the M−(CO) bond. The pyramidal geometry is predicted to be an energy minimum; the planar structure is the transition state for pyramidal inversion. Keeping θ constant (52°) and varying φ, we find the minimum at φ = 17°, with an inversion barrier of 1.2 kcal mol^{-1} (0.05 eV). In the planar geometry, the HOMO can be described as a nonbonding orbital localized on the metal. The pyramidalization contributes to delocalize this orbital on the $\{CO\}_2$ fragment, stabilizing the system. The evolution of the HOMO and the LUMO along the distortion coordinate is depicted in Figure 4.

Clearly, the HOMO−LUMO gap and, therefore, the inversion barrier, is intimately related to the chosen atomic parameter sets in EH calculations (see the Appendix). We carried out calculations with all transition metals from groups six through nine—$[CpCr(CO)_2]^-$ to $[CpIr(CO)_2]^{2+}$, except $[CpTc(CO)_2]$—and obtained the same qualitative picture in all cases. Interestingly, for $[CpCr(CO)_2]^-$, the HOMO and LUMO are inverted (vide infra), and the gap is smallest at 0.14 eV. For this compound, we accordingly find an inversion barrier of 11.3 kcal mol^{-1} (0.49 eV).

Full optimization of $[CpFe(CO)_2]^+$ with local and gradient-corrected DFT calculation yields a minimum energy for the pyramidalized geometry (Table 2). No minimum was localized for the planar geometry. Constraining the geometry to a planar one by fixing φ at 0°, and allowing the molecule to relax, we compute an inversion barrier of 10.46 kcal mol^{-1} (0.453 eV).

From the DFT-computed distances R(Fe−CO) and R(C−O) of Table 2, we note a clear-cut difference between the pyramidal and the planar structure. Consistent with the enhanced back-bonding and thus electron density shift from the metal into the CO ligand π*-system upon pyramidalization (which essentially is the physical driving force for going pyramidal), R(Fe−CO)

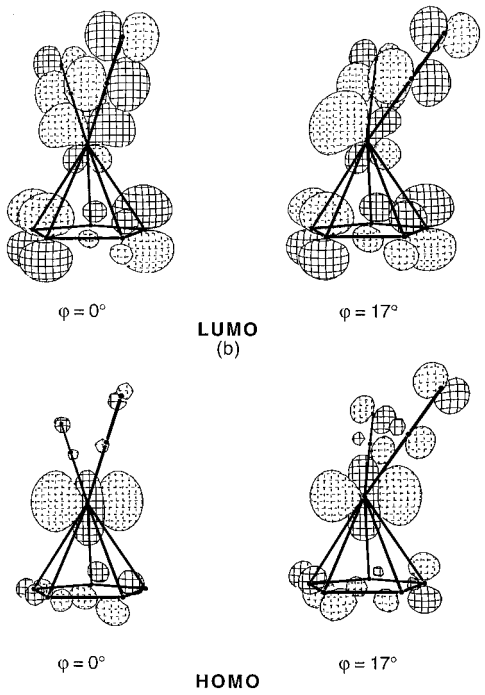

Figure 4. Evolution of the HOMO (a) and LUMO (b) of $[CpFe(CO)_2]^+$ along the pyramidalization reaction coordinate.

Table 2. Gradient-Corrected DFT Geometry Optimization of $[CpFe(CO)_2]^+$

	pyramidalized	planar (constrained)
rel energies (eV)	0.000	0.453
R(Fe−CO) (Å)	1.817	1.880
R(C−O) (Å)	1.147	1.143
$R(Cp_{centroid}-Fe)$ (Å)	1.729	1.705
φ (deg)	27.03	0
θ (deg)	47.07	51.51

is distinctly shorter and R(C−O) is slightly longer than in the planar case.

The same trend is seen in the reduced overlap populations for n(Mn−CO) and n(C−O) from our EH calculations of $[CpMn(CO)_2]$, which should correlate with the related bond distances. As reduced overlap populations n(C−O) in metal carbonyls usually also correlate with vibrational frequencies, we can compare the calculated values for the parent $[CpMn(CO)_3]$ (1.158, 1.157) with those computed for a planar (1.191) or pyramidal (1.151) fragment $[CpMn(CO)_2]$. We can relate these numbers to the experimentally observed CO frequencies of matrix-isolated $[CpMn(CO)_3]$ (2026, 1938 cm^{-1}). Clearly, a planar $[CpMn(CO)_2]$ structure should result in higher C−O stretching frequencies than those of $[CpMn(CO)_3]$. The experimental observation of smaller wavenumbers for the two C−O stretches corroborates stronger back-bonding and is consistent with a pyramidal geometry of $[CpMn(CO)_2]$ after CO loss from $[CpMn(CO)_3]$. Intensity measurements of observed vibrational absorptions ν_{CO} in the matrix also have allowed us to derive the interligand angle of OC−Mn−CO of matrix-isolated $[CpMn(CO)_2]$.[36,40] The value of 100° is in acceptable agreement with our computed value of 96.7° for pyramidal $[CpMn(CO)_2]$ in its minimum structure with $\theta = 54°$ and $\varphi = 22.5°$.

If improved back-bonding to π^*−MO's is indeed responsible for pyramidal ground-state geometries, substituting the COs for linear NOs, with lower lying π^*-acceptor orbitals, must increase the inversion barrier. For $[CpFe(NO)_2]^{3+}$, we compute a HOMO−LUMO gap of 0.17 eV for the planar geometry and an inversion barrier of 10.4 kcal mol^{-1} (0.45 eV) with optimal angles of $\theta = 54°$ and $\varphi = 20°$.

Inversion barriers in the range of 10−15 kcal mol^{-1} suggest that coordinatively unsaturated two-legged piano stool complexes with π-acidic ligands are pyramidal and may only be configurationally stable at very low temperature. Good candidates may also be systems with CS ligands, which are known to combine strong π acceptor with pronounced σ donor properties.

As the number of good π acceptor ligands is rather limited, we study systems that incorporate a good π acceptor and a pure σ donor. The most promising system will contain a high-lying lone pair on the σ donor, capable of interacting with the $d_{x^2-y^2}$ (HOMO), and a low-lying π acceptor orbital that can interact with the d_{xz} (LUMO). The best model candidate could be $[CpFe(SiH_3)NO]^+$. For the planar geometry, we compute a HOMO−LUMO gap of only 0.35 eV. The pyramidal structure is thus predicted to be an intermediate, with an inversion barrier of 6.9 kcal mol^{-1} (0.30 eV).

Let us now turn to Gladysz' building block: $[CpRePPh_3(NO)]^+$.[15−21] For the planar geometry, we compute a rather large HOMO−LUMO gap of 1.0 eV. The energy profile for the pyramidalization is fairly flat, but a shallow minimum is computed for $\theta = 53°$ and $\varphi = 15°$ with an inversion barrier of only 0.7 kcal mol^{-1} (0.03 eV). Although in the hands of Gladysz and coworkers the ligand substitution in enantiopure $[CpRe(PPh_3)(NO)L]^{x+}$ most often occurs with retention of configuration at the metal, we believe that the Jahn−Teller second-order distortion cannot be implied. Recently, Gladysz *et al.* suggested a possible associative mechanism to account for the retention of configuration upon ligand substitution.[41] Bending of the nitrosyl acts as an electron sink as two electrons are transferred into its π^*-orbital.[42,43] This relieves electron density from the formally twenty electron four-legged piano stool species; see eq 1. Such associative ligand substitution reactions via 20-electron species; have precedents in rhenium chemistry.[44]

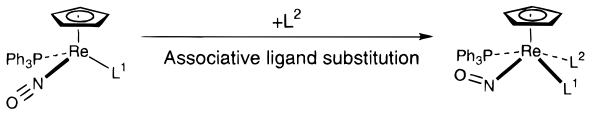

(1)

Several reports suggest that acyl-containing two-legged piano stool complexes incorporating a metal with d^6 electron count are configurationally stable.[4,45,50] A possibility that we investigate in this context is an η^2-coordination of the acyl fragment, as it is frequently found and has been theoretically analyzed for ground-

(40) Creaven, B. S.; Dixon, A. J.; Kelly, J. M.; Long, C.; Poliakoff, M. *Organometallics* **1987**, *6*, 2600.

(41) Dewey, M. A.; Zhou, Y.; Liu, Y.; Gladysz, J. A. *Organometallics* **1993**, *12*, 3924.

(42) Basolo, F.; Pearson, R. G. *Mechanisms of Inorganic Reactions. A Study of Metal Complexes in Solution*; John Wiley and Sons, Inc.: New York, 1967.

(43) Song, J.; Hall, M. B. *J. Am. Chem. Soc.* **1993**, *115*, 327.

(44) Casey, C. P. *Science* **1993**, *259*, 1552.

(45) Quinn, S.; Shaver, A.; Day, V. W. *J. Am. Chem. Soc.* **1982**, *104*, 1096.

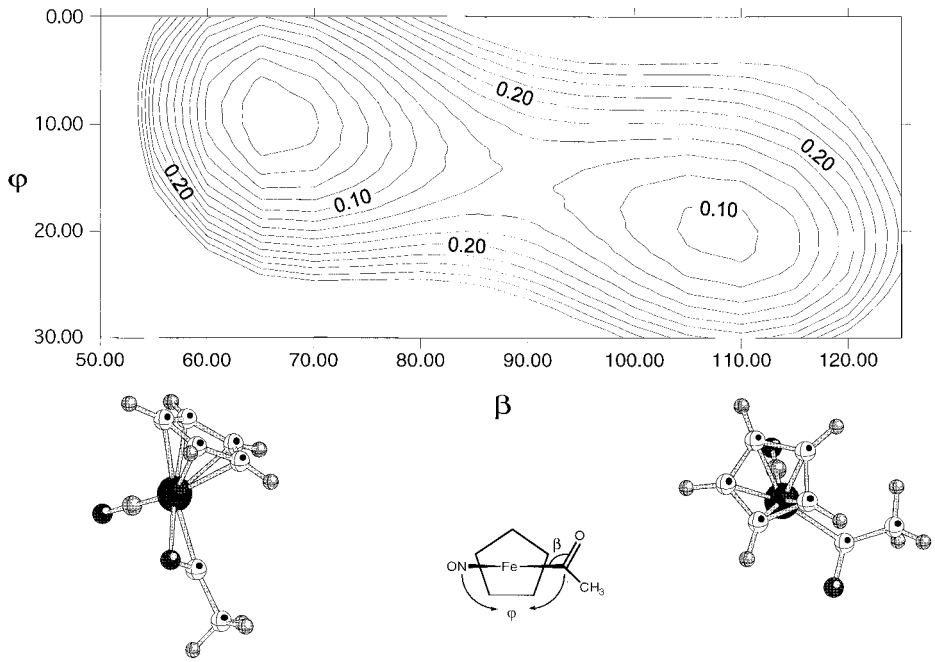

Figure 5. Potential energy surface for the $\eta^1-\eta^2$ interconversion of [CpFe(acyl)NO]$^+$ as a function of β and φ.

state structures in early transition-metal chemistry.[46] Such a coordination mode could explain the configurational stability during ligand substitution in a complex of the type [CpM(η^1-acyl)L^{1}L^2]. For such a process, the intermediate [CpM(η^2-acyl)L^2] can be regarded as coordinatively saturated and, therefore, account for the retention of configuration during ligand substitution, eq 2.

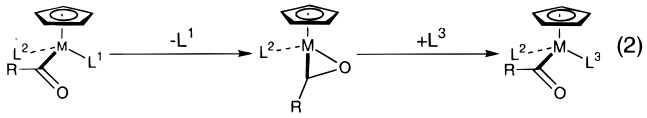

To our knowledge, d^6 {CpM(η^2-acyl)} systems have never been structurally characterized.[47] Related four-legged piano stool complexes with a d^4 electron count at the metal have been isolated and structurally characterized.[48,49]

We analyzed the model [CpFe(acyl)NO]$^+$. The presence of the NO$^+$ ligand favours pyramidalization and we compute a minimum at $\theta = 51°$, $\varphi = 20°$ and $\beta = 110°$, the latter being defined here as the Fe−C−O angle. Keeping θ as well as the dihedral angle O−C−Fe−Cp$_{centroid}$ and the Me−C−O angle constant at 51°, 270°, and 120°, respectively, we varied both φ and β. We find a second minimum corresponding to the η^2-geometry with $\varphi = 10°$ and $\beta = 65°$ (Figure 5). This latter is preferred by 2.3 kcal mol^{-1} (0.1 eV) over the coordinatively unsaturated species [CpFe(η^1-acyl)NO]$^+$. Interestingly, we find the presence of a good π acceptor essential for the location of a minimum for the η^2-coordination of an acyl. The nitrosyl relieves electron density from the metal, which makes it more electrophilic and thus favors η^2-coordination.

π Ligands: π Donors. To the best of our knowledge, the few isolable d^6 two-legged piano stool complexes reported to date contain ligands capable of π donation.[51−53] These all have a planar-at-metal geometry, and a recent analysis corroborates the results presented here.[33,54]

To illustrate this class of compounds, we studied [CpFeCl$_2$]$^-$. In addition to the previously described σ interactions, mostly with the d$_{yz}$ orbital and the sp hybrid, (Figure 2), the occupied d$_{z^2}$ (HOMO) and d$_{xy}$ orbitals (HOMO-1) of {CpFe}$^+$, as well as the empty d$_{xz}$ orbital (LUMO), are all destabilized upon interaction as they mix out-of-phase with the symmetry-adapted combinations of filled, low-lying p-orbitals of the electronegative ligands. As both HOMO and LUMO are destabilized, the HOMO−LUMO gap (1.2 eV) remains too big to allow for efficient mixing. A Walsh diagram confirms that the planar geometry is the preferred one. Calculations for [CpMnCl$_2$]$^{2-}$ yield identical results.

Recently, Kölle *et al.* published the X-ray structure of a bent two-legged piano stool 16-electron complex: [Cp*Ru(acac)] (Cp* = C$_5$Me$_5$; acac = acetylacetonato).[55] Eventually, it was shown that this bent geometry was caused by an interaction of the coordinatively unsaturated ruthenium center with the π-system of another acac at the central methine carbon. Kölle's compound is thus best described as a dimer with effective [CpML$_3$] structure of each Ru in the solid state: [Cp*Ru(acac)]$_2$ **A**.[56] We carried out extended Hückel calculations on the monomeric system [CpRu(acac)] and find that the planar geometry is favored by 6.9 kcal mol^{-1} (0.30 eV)

(46) Tatsumi, K.; Nakamura, A.; Hofmann, P.; Stauffert, P.; Hoffmann, R. *J. Am. Chem. Soc.* **1985**, *107*, 4440.
(47) Durfee, L. D.; Rothwell, I. P. *Chem. Rev.* **1988**, *88*, 1059.
(48) Curtis, M. D.; Shiu, K.-B.; Butler, W. M. *J. Am. Chem. Soc.* **1986**, *108*, 1550.
(49) Adams, R. D.; Chodosh, D. F. *J. Am. Chem. Soc.* **1977**, *99*, 6544.
(50) Brunner, H.; Vogt, H. *Angew. Chem., Int. Ed. Engl.* **1981**, *20*, 405; *Angew. Chem.* **1981**, *93*, 409.
(51) Campion, B. K.; Heyn, R. H.; Tilley, T. D. *Chem. Commun.* **1988**, 278.
(52) Johnson, T. J.; Huffman, J. C.; Caulton, K. G. *J. Am. Chem. Soc.* **1992**, *114*, 2725.
(53) Bursten, B. E.; Gatter, M. G.; Goldberg, K. I. *Polyhedron* **1990**, *9*, 2001.
(54) Bickford, C. C.; Johnson, T. J.; Davidson, E. R.; Caulton, K. G. *Inorg. Chem.* **1994**, *33*, 1080.
(55) Kölle, U.; Kossakowski, J.; Raabe, G. *Angew. Chem., Int. Ed. Engl.* **1990**, *29*, 773; *Angew. Chem.* **1990**, *102*, 839.
(56) Smith, M. E.; Hollander, F. J.; Andersen, R. A. *Angew. Chem., Int. Ed. Engl.* **1993**, *32*, 1294; *Angew. Chem.* **1993**, *105*, 1355.

over the bent one. As for the $[CpFeH_2]^-$ diagram, the total energy follows closely the fate of the d_{xy} orbital.

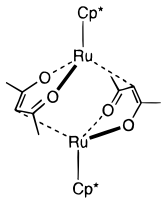

A

Cyclopolyenyl Ligand Effects. The above-mentioned 16-electron fragments $[CpFe(CO)_2]^+$ or $[CpMn(CO)_2]$ are not only versatile building blocks and useful reactive intermediates in organometallic synthesis but also represent members of a broad isoelectronic series of 16-electron half-sandwich dicarbonyls with variable ring size of the cyclopolyenyl ligand and accordingly varied metal centers and charges. If we stay with neutral systems $[(\eta^n\text{-}C_nH_n)M(CO)_2]$, the Cp ligand of $[CpMn(CO)_2]$ can be replaced by $\eta^4\text{-}C_4H_4$, $\eta^6\text{-}C_6H_6$, or $\eta^7\text{-}C_7H_7$, if the metal changes to Fe, Cr, and V, respectively. Like $[CpMn(CO)_3]$, the 18-electron three-legged piano stool complexes $[(\eta^4\text{-}C_4H_4)Fe(CO)_3]$, $[(\eta^6\text{-}C_6H_6)Cr(CO)_3]$, and $[(\eta^7\text{-}C_7H_7)V(CO)_3]$ are of course all well-known and are potential precursors for the (e.g., photochemical) generation of the related unsaturated $[(\eta^n\text{-}C_nH_n)M(CO)_2]$ species.[32,57−60] Their electronic structures and geometries will be briefly discussed here.

We have not studied three- and eight-membered ring systems, i.e., $[(\eta^3\text{-}C_3H_3)Co(CO)_2]$ and $[(\eta^8\text{-}C_8H_8)Ti(CO)_2]$, because the Co system, for which parent tricarbonyl complexes $[(\eta^3\text{-}C_3R_3)Co(CO)_3]$ are known, can be extrapolated from the others, and for the Ti half-sandwich we do not expect a planar $(\eta^8\text{-}C_8H_8)^{2-}$ ligand with its large perimeter to match the bonding requirements of a single, small Ti^{2+} center.

We performed analogous model calculations as detailed above for $[CpFe(CO)_2]^+$ or $[CpMn(CO)_2]$ and their other Cp-congeners for the benzene complex $[(\eta^6\text{-}C_6H_6)Cr(CO)_2]$, simultaneously optimizing angles θ and φ. The resulting energy surface $E = E(\theta,\varphi)$ was virtually identical to the $[CpMn(CO)_2]$ and $[CpFe(CO)_2]^+$ cases. A detailed analysis shows that the same electronic structure characteristics apply, which were already described for the Cp systems. The planar geometry displays a small HOMO−LUMO gap of 0.34 eV, which opens widely upon pyramidalization. For our metal Cr parameters, the HOMO and LUMO of the planar $[(\eta^6\text{-}C_6H_6)Cr(CO)_2]$ geometry, as for $[CpCr(CO)_2]^-$, have interchanged their role compared to $[CpMn(CO)_2]$. Of course, the second-order Jahn−Teller arguments still apply and are responsible for the pyramidal ground state.

Interestingly, the situation changes upon going to either $[(\eta^4\text{-}C_4H_4)Fe(CO)_2]$ or to $[(\eta^7\text{-}C_7H_7)V(CO)_2]$. In both cases only extremely shallow, very weakly pyramidal minima are found. Table 3 shows the computed results for all four systems. The negligible tendency toward pyramidalization for $[(\eta^4\text{-}C_4H_4)Fe(CO)_2]$ and $[(\eta^7\text{-}C_7H_7)V(CO)_2]$ reflects the much larger HOMO−LUMO gaps that we calculate for these two 16-electron systems, different from the Cp and benzene complexes. $[(\eta^4\text{-}C_4H_4)Fe(CO)_2]$ reveals a HOMO−LUMO ordering (d_{xz} above d_{z^2}) as $[CpFe(CO)_2]^+$ or $[CpMn(CO)_2]$, while $[(\eta^7\text{-}C_7H_7)V(CO)_2]$ displays the reverse order like $[(\eta^6\text{-}C_6H_6)Cr(CO)_2]$.

Table 3. Computed Geometries and Energies of $[(\eta^n\text{-}C_nH_n)M(CO)_2]$ Systems

$[(\eta^n\text{-}C_nH_n)M(CO)_2]$	planar θ (deg)	pyramidal θ (deg)	pyramidal φ (deg)	E_{inv} (kcal mol^{-1})
$[(\eta^4\text{-}C_4H_4)Fe(CO)_2]$	54	54	10	0.3
$[(\eta^5\text{-}C_5H_5)Mn(CO)_2]$	51	54	22.5	8.5
$[(\eta^6\text{-}C_6H_6)Cr(CO)_2]$	45	50	21	8.0
$[(\eta^7\text{-}C_7H_7)V(CO)_2]$	45	50	10	0.1

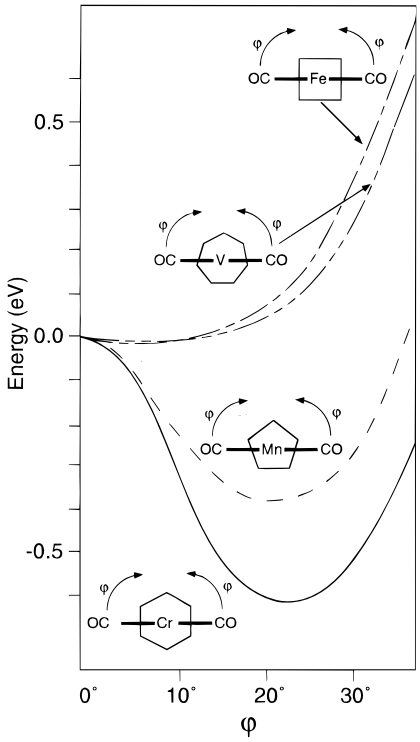

Figure 6. Computed total energy curves $E = E(\varphi)$ [with θ kept constant at 54°] for a planar to pyramidal distortion of the four $[(\eta^n\text{−}C_nH_n)M(CO)_2]$ 16-electron fragments in comparison.

Figure 6 shows computed total energy curves $E = E(\varphi)$ [with θ kept constant at 54°] for a planar to pyramidal distortion of the four $[(\eta^n\text{-}C_nH_n)M(CO)_2]$ 16-electron complexes in comparison.

To understand the difference between the Mn, Fe^+, Cr, and Fe, V systems, respectively, it is necessary to inspect more closely the two frontier orbitals, which in our previous cases $[CpMn(CO)_2]$, $[CpFe(CO)_2]^+$, and $[(\eta^6\text{-}C_6H_6)Cr(CO)_2]$, due to a small HOMO−LUMO gap and the concomitant second-order Jahn−Teller instability for the planar geometry, were responsible for keeping these unsaturated molecules pyramidal. So far, we have not dwelled upon the fact that these two Mo's (see Figure 4) obviously also contain contributions to their wavefunctions, which stem from the cyclopolyenyl ring system. These contributions have been omitted in our simplified pictorial representation of the valence Mo's of the $\{CpFe\}^+$ fragment in Figures 1 and 2, where only the dominant metal contributions, responsible for metal−

(57) Campen, A. K.; Narayanaswamy, R.; Rest, A. J. *J. Chem. Soc., Dalton Trans.* **1990**, 823.
(58) Hill, R. H.; Wrighton, M. S. *Organometallics* **1985**, *4*, 413.
(59) Hill, R. H.; Wrighton, M. S. *Organometallics* **1987**, *6*, 632.
(60) Oishi, S. *J. Orgamomet. Chem.* **1987**, *335*, 207.

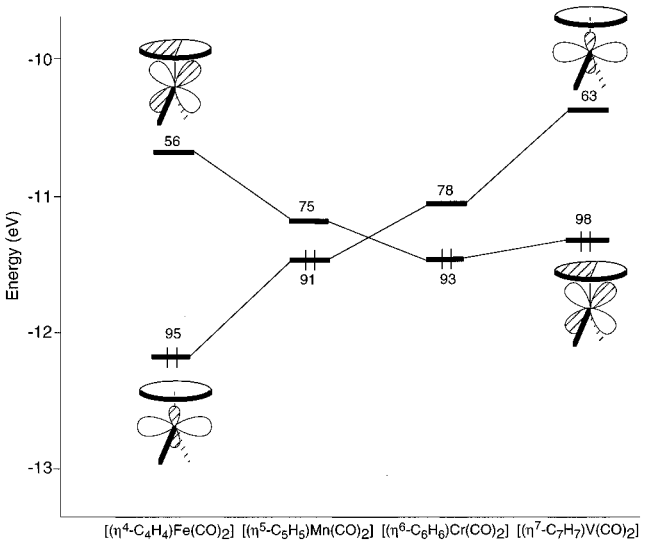

Figure 7. Frontier orbitals for the series $[(\eta^n\text{-}C_nH_n)M(CO)_2]$ ($n = 4-7$; M = Fe, Mn, Cr, V). The numbers indicate the contribution (in %) of the $\{M(CO)_2\}$ fragment.

CO interactions, are displayed. If we want to discuss the influence of the cyclopolyenyl ring along the isoelectronic Fe to V series, however, we have to take into account that the frontier orbital with mainly d_{z^2} character at the metal (the HOMO for planar $[(\eta^4\text{-}C_4H_4)Fe(CO)_2]$, $[CpMn(CO)_2]$, and $[CpFe(CO)_2]^+$ and the LUMO for planar $[(\eta^6\text{-}C_6H_6)Cr(CO)_2]$ and $[(\eta^7\text{-}C_7H_7)V(CO)_2]$) contains an antibonding contribution from the lowest lying, totally symmetric π-orbital of the C_nH_n ligand (with facial σ-symmetry toward the η^n-bound $M(CO)_2$ moiety, viz. a_2'' of Cp^- in Figure 1) to its MO wavefunction. Correspondingly, the other frontier MO with d_{xz} character at the metal (the LUMO for planar $[(\eta^4\text{-}C_4H_4)Fe(CO)_2]$, $[CpMn(CO)_2]$ and $[CpFe(CO)_2]^+$ and the HOMO for planar $[(\eta^6\text{-}C_6H_6)Cr(CO)_2]$, and $[(\eta^7\text{-}C_7H_7)V(CO)_2]$) carries a $\eta^n\text{-}C_nH_n$ ring contribution, which originates from the appropriate member of the lowest lying e-set of the cyclopolyenyl ring system (of π-symmetry toward the $\eta^n\text{-}C_nH_n\text{-}M(CO)_2$ moiety, viz. e_1'' of Cp^- in Figure 1). In Figure 7, the HOMO−LUMO situation for the planar $d^6\text{-}[(\eta^n\text{-}C_nH_n)M(CO)_2]$ species is depicted, the cyclopolyenyl ligand contributions to the frontier MOs are sketched, and is the localization in percent of the wavefunction at the respective $\{M(CO)_2\}$ unit, and thereby also at the cyclopolyenyl ring, is also given.

The computed changes in $M(CO)_2$ vs. ring localization of the HOMO and LUMO wavefunctions, the ascent of the d_{z^2}-based level, the descent of the d_{xz}-derived MO, and the level crossing upon going from left to right can be readily traced back to two main trends. Going from Fe to V decreases the metal's electronegativity, and as a consequence, the d_{z^2} MO rises in energy. Simultaneously, however, the variation of the cyclopolyenyl perimeter from C_4H_4 via benzene and Cp to C_7H_7 makes the lowest lying e-set of ring π-orbitals come down in energy, as already visible from simple Hückel theory [$\epsilon_{HMO} = \alpha, \alpha + 0.618\,\beta, \alpha + \beta, \alpha + 1.247\,\beta$].[39] These two effects lead to the orbital energy trends shown in Figure 7. For all systems, the HOMO remains mostly localized on the metal and is essentially a nonbonding electron pair at the metal center. The LUMO, in all cases, has an appreciable admixture of ring character. In $[(\eta^4\text{-}C_4H_4)Fe(CO)_2]$, Figure 7 left, this admixture stems from the e-set component of the C_4H_4 π-system, while for $[(\eta^7\text{-}C_7H_7)V(CO)_2]$, Figure 7 right, it stems from the lowest a-type π-MO of C_7H_7.

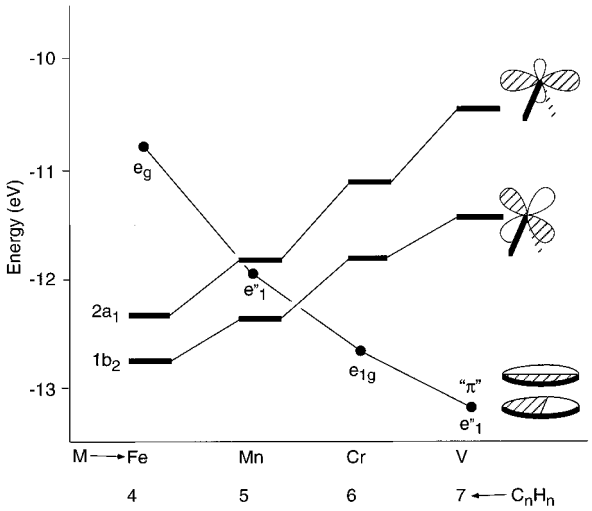

Figure 8. Energy of $\{M(CO)_2\}$ orbitals (M = Fe, Mn, Cr, V) and of the lowest lying π-orbital e-set of the C_nH_n series ($n = 4-7$).

It may be easier to visualize and understand the trends discussed here if we construct the orbitals of the planar $[(\eta^n\text{-}C_nH_n)M(CO)_2]$ complexes not from the conical fragments $\{(\eta^n\text{-}C_nH_n)M\}$, each interacting with the $(CO)_2$ ligand set as we have done so far (see Figure 2), but if we alternatively use the MOs of each $\{M(CO)_2\}$-fragment, interacting with the respective π-ring system. The valence MOs of a bent fragment $\{M(CO)_2\}$ are well-known.[39] Together with the energy position of the lowest lying e-set MO along the C_nH_n series (e_g, e_1'', e_{1g}, e_1''), Figure 8 depicts those two levels of each $M(CO)_2$ unit, $1b_2$ and $2a_1$, from which the HOMO and LUMO orbitals of Figure 7 are derived.

In this picture, the d_{z^2}-derived frontier MOs in Figure 7 originate from the $2a_1$ fragment MOs of Figure 8, with a small antibonding admixture of the lowest π-MO of the rings, and the levels with d_{xz} character in Figure 7 are derived from the antibonding combination of each metal fragment's $1b_2$ MO and the symmetry matching component of the C_nH_n e-set shown in Figure 8. The opposite slope of the two subsets of fragment orbitals—the mostly electronegativity-based ascent of the metal levels and the perimeter dependent descent of the ring e-set—then makes the resulting frontier MO situation of Figure 7 obvious.

Only for the Cp and benzene derivatives in the center of the diagram, the match of metal and ring orbitals creates a HOMO−LUMO gap small enough to make the planar 16-electron fragments sufficiently unstable in a second-order Jahn−Teller sense, thus inducing pyramidal geometries.

Conclusion

Although the possibility exists to stabilize pyramidal 16-electron two-legged piano stool complexes, caution must be applied in the choice of the ligands. The most promising candidates at least for Cp and benzene complexes should contain good π-accepting ligands, which should be good σ-donors as well. Pure σ- and π-donors will favor a planar geometry. Even in the best cases, where the pyramidal geometry is predicted to be an intermediate rather than a transition state, we

compute an inversion barrier that can be overcome at room temperature in solution. However, we must bear in mind that, during a ligand substitution, there will be two competing reactions: the racemization and the ligand substitution. If the substitution rates are higher than the racemization rates, retention of configuration may result, although the inversion barriers are low.

Perhaps the most promising three-legged piano stool complexes for catalytic applications should contain ligands capable of adapting their coordination mode to the electronic needs of the metal. Nitrosyls that can bend and thus allow for associative ligand substitution are candidates. Ring slippage for indenyls and cyclopentadienyl-containing complexes has also received considerable attention.[61] Acyls that can bind via an η^2-mode, thus allowing a dissociative ligand substitution pathway to proceed via a coordinatively saturated intermediate, have been shown to be a possibility. Similarly, agostic interactions have been demonstrated to temporarily occupy a vacant site during ligand substitution.[62,63]

As discussed for the series of unsaturated dicarbonyl half-sandwich fragments $[(\eta^n\text{-}C_nH_n)M(CO)_2]$, it is also important to note that the ring size of the cyclopolyenyl ligands and the positioning of the metal in the periodic table may have a distinct influence upon the potential configurational stability and inversion barriers of 16-electron two-legged piano stool complexes.

Appendix

All extended Hückel calculations[64−66] were carried out with the CACAO[67] or FORTICON 8[79] program systems. The parameters were all taken from previous work and are listen in Table 4. Apart from [Cp*Ru(acac)], where distances were taken from the original X-ray data, all other distances were taken from ref 68: C−C 1.40 Å, C−H 1.05 Å, N−H 1.00 Å, Fe−H 1.61 Å, Fe−SiH_3 2.33 Å, Fe−PH_3 2.24 Å, Fe−CO 1.78 Å, C−O 1.15 Å, Fe−C_{acyl} 2.02 Å, C_{acyl}−O 1.20 Å, C−CH_3 1.5 Å, Fe−NO 1.67 Å, N−O 1.17 Å, Fe−Cl 2.26 Å, Fe−NH_2 2.04 Å, Re−PH_3 2.42 Å, Re−NO 1.75 Å, Re−Cp 1.96 Å, Mn−H 1.60 Å, Mn−CO 1.80 Å, Mn−P 2.24 Å, Mn−Cl 2.0 Å, M−C_{CnHn} 2.15 Å (M = Fe, Mn, Cr, V; $n = 4-7$), C−C_{CnHn} 1.40 Å, C−H_{CnHn} 1.05 Å ($n = 4-7$).

The DFT calculations were carried out with the program system ADF (Version 1.1.3), developed by Baerends *et al.*[69,70] Te Velde *et al.* developed the numerical integration procedure.[71,72] The atomic orbitals on iron, carbon, and oxygen were described by an uncontracted triple-ζ STO basis set. A polarization function was added for C, H, and O. The $1s^2$ configuration on carbon and oxygen as well as the $1s^22s^22p^6$ configuration of iron were assigned to the core and treated by the frozen-core approximation.[70,73] A set of auxiliary s, p, d, f, g functions, centered on all nuclei, was used to fit electron density together with both Coulomb and exchange potentials in each SCF cycle.[74] All optimized geometries in this study were based on the energy expression from the local density approximation (LDA) augmented with Becke's approximation for the exchange and Perdew's for the correlation. These nonlocal corrections were included self-consistently.[75−78]

Table 4. Parameters Used in Extended Hückel Calculations

atom	orbital	H_{ii} (eV)	ζ_1	ζ_1	c_1	c_2
Fe	3d	−12.70	5.35	1.80	0.5366	0.6678
	4s	−9.17	1.90			
	4p	−5.37	1.90			
Mn	3d	−12.01	5.15	1.70	0.5193	0.6929
	4s	−9.66	1.90			
	4p	−4.94	1.90			
Cr	3d	−11.23	4.95	1.60	0.4876	0.7205
	4s	−9.38	1.70			
	4p	−5.30	1.70			
V	3d	−10.48	4.75	1.50	0.4558	0.7516
	4s	−9.17	1.60			
	4p	−5.46	1.60			
Re	5d	−12.66	5.34	2.28	0.6662	0.5910
	6s	−9.36	2.40			
	6p	−5.96	2.37			
Ru	4d	−12.20	4.21	1.95	0.5772	0.5692
	4s	−8.00	2.08			
	4p	−4.30	2.04			
P	3s	−18.60	1.60			
	3p	−14.00	1.60			
Si	3s	−17.30	1.38			
	3p	−9.20	1.38			
C	2s	−21.40	1.63			
	2p	−11.40	1.63			
N	2s	−26.00	1.95			
	2p	−13.40	1.95			
O	2s	−32.30	2.28			
	2p	−14.80	2.28			
Cl	3s	−26.30	2.18			
	3p	−14.20	1.73			
H	1s	−13.60	1.30			

Acknowledgment. Financial support for T.R.W. was provided by the Swiss National Science Foundation and the Stiftung für Stipendien auf dem Gebiete der Chemie (Werner Fellowship (1994−1998)).

OM9700369

(61) O'Connor, J. M.; Casey, C. P. *Chem. Rev.* **1987**, *87*, 307.
(62) Cracknell, R. B.; Orpen, A. G.; Spencer, J. L. *Chem. Commun.* **1986**, 1005.
(63) Brookhart, M.; Lincoln, D. M.; Volpe, A. F. J.; Schmidt, G. F. *Organometallics* **1989**, *8*, 1212.
(64) Hoffmann, R.; Lipscomb, W. N. *J. Chem. Phys.* **1962** , *36*, 2179.
(65) Hoffmann, R. *J. Chem Phys.* **1963**, *39*, 1397.
(66) Ammeter, J. H.; Bürgi, H.-B.; Thibeault, J. C.; Hoffmann, R. *J. Am. Chem. Soc.* **1978**, *100*, 3686.
(67) Mealli, C.; Proserpio, D. M. *J. Chem. Educ.* **1990**, *67*, 399.
(68) Orpen, A. G.; Brammer, L.; Allen, F. H.; Kennard, O.; Watson, D. G.; Taylor, R. *J. Chem. Soc., Dalton. Trans.* **1989**, S1.
(69) ADF, Amsterdam Density functional, Department of Theoretical Chemistry, Vrije Universiteit, De Boelelaan 1083, 1081 HV Amsterdam, The Netherlands, 1994.
(70) Baerends, E. J.; Ellis, D. E.; Ros, P. *Chem. Phys.* **1973**, *2*, 41.
(71) Boerrigter, P. M.; Te Velde, G.; Baerends, E. J. *Int. J. Quantum Chem.* **1988**, *33*, 87.
(72) te Velde, G.; Baerends, E. J. *J. Comput. Phys.* **1992**, *99*, 84.
(73) Ravenek, W. *Algorithms and Applications on Vector and Parallel Computers*; Elsevier: Amsterdam, 1987.
(74) Krijn, J.; Baerends, E. J. Fit functions in the HFS-method; Free University of Amsterdam: Amsterdam, 1981.
(75) Perdew, J. P. *Phys. Rev. B* **1986**, *33*, 8822.
(76) Perdew, J. P. *Phys. Rev. B* **1986**, *34*, 7406.
(77) Vosko, S. H.; Wilk, L.; Nusair, M. *Can. J. Phys.* **1980**, *58*, 1200.
(78) Becke, A. D. *Phys. Rev. A* **1988**, *38*, 3098.
(79) Howell, J.; Rossi, A.; Wallace, D.; Haraki, K.; Hoffmann, R. Quantum Chemical Program Exchange, QCPE No. 334.